Associated conference: 5th International Small Sample Test Techniques Conference

Conference location: Swansea University, Bay Campus

Conference date: 10th - 12 July 2018

How to cite: Bruchhausen, M. Altstadt, E., Austin, T. Dymacek, P., Holmström, S., Jeffs, S., Lacalle, R., Lancaster, R., Matocha, K., Petzova, J. 2018. European standard on small punch testing of metallic materials. *Ubiquity Proceedings*, 1(S1): 11 DOI: https://doi.org/10.5334/uproc.11

Published on: 10 September 2018

UBIQUITY PROCEEDINGS

ubiquity press open access https://ubiquityproceedings.com

European standard on small punch testing of metallic materials

M. Bruchhausen [1,*], E. Altstadt [2], T. Austin [3], P. Dymacek [4], S. Holmström [5], S. Jeffs [6], R. Lacalle [7], R. Lancaster [8], K. Matocha [9], and J. Petzova [10]

[1] European Commission, JRC, 1755 LE Petten, The Netherlands; matthias.bruchhausen@ec.europa.eu
[2] Helmholtz-Zentrum Dresden-Rossendorf, 01328 Dresden, Germany; e.altstadt@hzdr.de
[3] European Commission, JRC, 1755 LE Petten, The Netherlands; simon.austin@ec.europa.eu
[4] Institute of Physics of Materials AS CR, 61662 Brno, Czech Republic; pdymacek@ipm.cz
[5] European Commission, JRC, 1755 LE Petten, The Netherlands; stefan.holmstrom@ec.europa.eu
[6] Institute of Structural Materials, Swansea University, SA1 8EN Swansea, United Kingdom; s.p.jeffs@swansea.ac.uk
[7] Inesco Ingenieros, Santander, 39005 Spain; lacaller@inescoingenieros.com
[8] Institute of Structural Materials, Swansea University, SA1 8EN Swansea, United Kingdom; r.j.lancaster@swansea.ac.uk
[9] Faculty of Metallurgy and Materials Engineering, VŠB-Technical University of Ostrava, 70833 Ostrava, Czech Rep; matocha.karel@email.cz
[10] VUJE, 91864 Trnava, Slovak Republic; jana.petzova@vuje.sk

***** Correspondence: matthias.bruchhausen@ec.europa.eu; Tel.: +31-224-565218

Abstract: In the 1980s, studying the effect of neutron irradiation and temper embrittlement on structural materials for the fusion and fission programmes was a major challenge. In this context the development of small specimen test techniques began, allowing the characterization of structural materials for nuclear applications with small amounts of material. The small punch technique is of one these small specimen test approaches. It is widely used for the development and monitoring of structural materials, however there is currently no comprehensive international standard for small punch testing. An EN standard on small punch testing is currently being developed under the auspices of ECISS/TC101/WG1. Besides describing the apparatus, procedures, and specimens, it will include recommendations for the estimation of tensile, fracture and creep properties from small punch testing as well as machine readable formats for representing and transferring test data.

This paper describes the current status of the standard and highlights some of the changes with regard to the current CWA 15672 (2007).

Keywords: small punch test, standard

1. Introduction

The need for the characterization of irradiated materials for the fission and fusion programs has led to much research into small specimen test techniques [1]. These test techniques have received much interest especially for nuclear applications because they reduce the exposure of staff to radiation, the cost of irradiation experiments and the amount radioactive waste.

The small punch (SP) technique is a small specimen test technique which has received much interest since its introduction in the 1980s in the fusion and fission programs for structural alloys mainly in the U.S. and Japan [2-7].

Nowadays, the SP technique is used for the characterization of structural materials for nuclear power plants [8,9]. It is more and more also being used in other industries like aerospace [10,11], automotive [12] or off-shore [13] and for non-metallic materials like polymers [14] or bones [15].

Despite this increasing use of the SP test there is currently no international standard covering the most relevant aspects of small punch testing. National standards or other guidance documents exist in some countries [16-18] or are under preparation [19]. The most recent European guidance is the CEN Workshop Agreement (CWA) 15627, a pre-normative document [20]. An EN standard "Metallic materials - Small punch test method" is currently being formulated under the auspices of ECISS/TC101/WG1[1]. This standard will cover the estimation of tensile and fracture mechanics properties from cryogenic to high temperatures from SP testing as well as address the estimation of uniaxial creep properties from small punch creep (SPC) data.

[1]Working Group (WG) 1 of the Technical Committee (TC) 101 "Test methods for steel (other than chemical analysis)" within the European Committee for Iron and Steel Standards (ECISS)

This article gives an overview of the most important points of the new standard and highlights some of the differences to the current CWA 15627. Note however that at the time of writing the public enquiry phase of the standardization process has not yet started. It may well be that the public enquiry will lead to changes in the standard.

2. Principle of SP testing

In an SP or SPC test, a punch with a hemispherical tip or a ball is pushed through a disc specimen along its axis (Figure 1). The SP test is displacement-controlled, i.e. the punch is pushed with constant velocity of the cross head w through the specimen and the force F required to keep the punch moving is measured as a function of punch displacement v (at the punch tip) or specimen deflection u (measured on the lower side of the specimen, opposite to the contact point between punch and specimen).

In contrast the SPC test is force-controlled, i.e. the punch is pressed with constant force on the specimen and the displacement v or deflection u are measured as a function of time t.

Typical examples of an SP and an SPC curve are shown in Figure 2 (a) and (b).

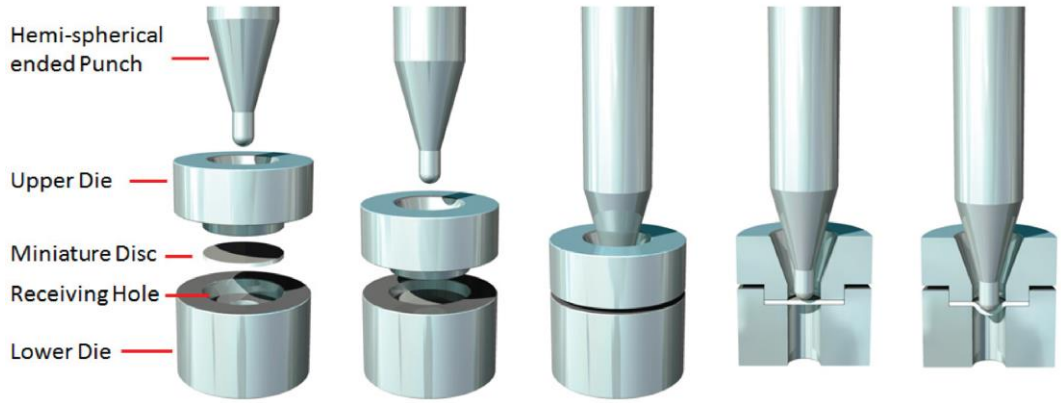

Figure 1. Schematic of a SP test [21].

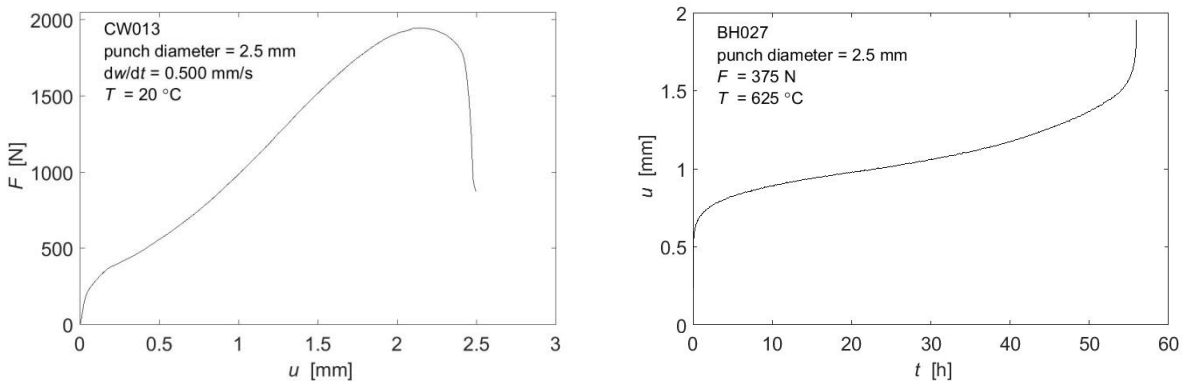

(a) (b)

Figure 2. (a) Force-deflection curve from an SP test [22] and **(b)** creep-deflection curve from a SPC test [23].

3. Scope and structure of the new EN standard

The new EN standard specifies the equipment and procedures for carrying out SP and SPC tests of metallic materials. Its informative annexes give guidance for estimating tensile, fracture mechanical and creep material properties.

The standard has the following clauses:

1. Introduction
2. Scope

3. Normative references
4. Terms and definitions
5. Symbols and designations
6. Test piece
7. Material sampling
8. Small punch test
9. Small punch creep test

And the informative annexes:

A. Determining the compliance of a small punch test rig for displacement measurements
B. Procedure for temperature and measurement during small punch testing
C. Estimation of ultimate tensile strength R_m from small punch testing
D. Estimation of proof strength $R_{p0,2}$ from small punch testing
E. Estimation of DBTT from small punch testing
F. Fracture toughness from small punch testing
G. Estimation of creep properties from small punch creep testing
H. Post-test examination of the test piece
I. Machine readable formats

4. Test piece and test rig

The new standard allows two types of specimen: besides the most frequently used "standard" specimen with a diameter D_S of 8 mm and an initial thickness h_0 of 0.5 mm also "miniature" TEM sample sized specimens may be used where D_S=3 mm, h_0=0.25 mm. However, since there is less experience with the miniature SP specimen, in some cases the more detailed recommendations are given for the larger specimen only.

The preparation of the test pieces follows the same lines as the CWA 15627.

For the test rig, CWA 15627 specifies a punch tip radius r = 1.25 mm for SP tests and a range of r = 1.00-1.25 mm for SPC tests. The new standard stipulates a common r for each specimen size for SP and SPC testing (Table 1).

During the test, the specimen is clamped between an upper and a lower die. The lower die has a receiving hole with diameter D and a chamfer of length L. Both, D and L depend on the type of specimen used (Figure 3, Table 1).

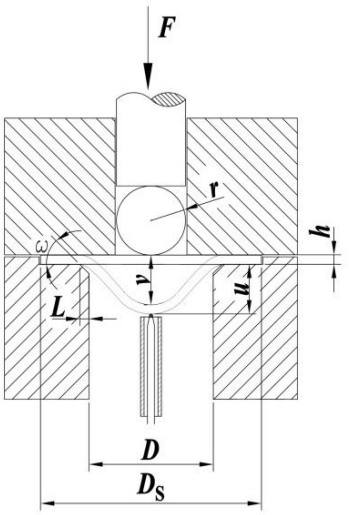

Figure 3. Sketch indicating the main geometrical denominations.

Table 1. Main geometric characteristics of the SP/SPC rig for standard (D_S=8 mm) and miniature specimens (D_S=3 mm).

Test piece	***D* [mm]**	***r* [mm]**	***L* [mm]**
Standard	4	1.25	0.2
Miniature	1.75	0.5	0.2

5. Estimation of material properties

While the provisions with regard to the test piece, the rig, and the test itself remain largely the same as in the CWA 15627, the recommendations in the informative annexes with regard to data evaluation have in some cases been changed and extended quite significantly.

5.1. Estimation of proof stress

Estimates of proof strength $R_{p0.2}$ are obtained from SP data by correlating them to characteristic points on the force deflection curve [24,25]:

$$R_{p0.2} = \beta_{Rp0.2} \frac{F_3}{h_0^2}, \tag{1}$$

where F_e is the elastic-plastic transition force and $\beta_{Rp0,2}$ is an empirical correlation coefficient which depends on the geometry of the test rig.

The new standard maintains equation (1) for relating $R_{p0,2}$ to F_e. Several approaches for determining F_e are discussed in the literature [24,25]. If displacement data is used, the new standard uses the same bilinear fit included in the CWA 15627:

$$f(u) = \begin{cases} \frac{f_A}{u_A} u & \text{for} \quad 0 \le u < u_A \\ \frac{f_B - f_A}{u_B - u_A}(u - u_A) + f_A & \text{for} \quad u_A \le u \le u_B \end{cases} \tag{2}$$

The fitting parameters f_A, f_B and u_A are determined by minimizing the error:

$$err = \int_0^{u_B} [F(u) - f(u)]^2 \, du. \tag{3}$$

The standard defines F_e directly as the intersection point f_A (i.e. F_e=f_A, Figure 4 (a)) whereas the CWA 15627 used the projection of f_A on the curve $F(u)$ (i.e. F_e=$F(u_A)$. The changes were made because data from a round robin exercise showed less scatter for f_A than for $F(u_A)$. If punch displacement v is used rather than specimen deflection u, a very similar trilinear fit (Figure 4 (b)) is used which is defined as:

$$f(v) = \begin{cases} 0 & \text{for} \quad 0 \le v < v_0 \\ \frac{f_A}{v_A - v_0}(v - v_0) & \text{for} \quad v_0 \le v < v_A \\ \frac{f_B - f_A}{v_B - v_A}(v - v_A) + f_A & \text{for} \quad v_A \le v \le v_B \end{cases} \tag{4}$$

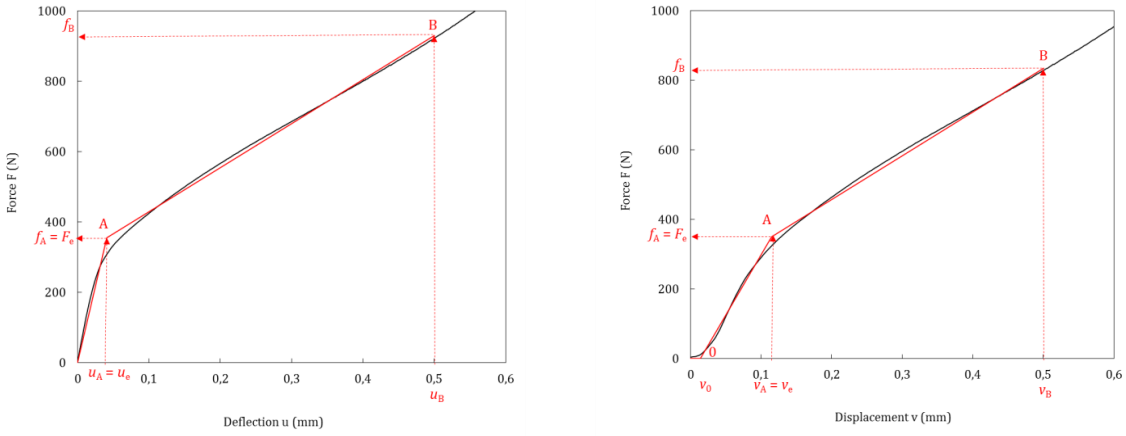

(a) (b)

Figure 4. Determination of F_e by **(a)** bilinear method from a force-deflection curve and **(b)** by trilinear method from a force-displacement curve.

The recommended values for $\beta_{Rp0,2}$ for the standard 8 mm specimen are given in Table 2.

Table 2. Proposed $\beta_{Rp0.2}$ values for standard test piece and standard device configuration (steels with $R_{p0.2}$ between 200 and 1000 MPa).

Test piece	**Curve type**	$\boldsymbol{\beta_{Rp0.2}}$
Standard (8 mm)	$F(u)$	0.510
Standard (8 mm)	$F(v)$	0.479

5.2 Estimation of utlimate tensile strength

For estimating the ultimate tensile strength R_m most authors use correlations between R_m and F_m very similar to that for $R_{p0,2}$ (Equation 1) The best results are obtained by [25]:

$$R_m = \beta_{Rm} \frac{F_m}{h_0 u_m,} \tag{5}$$

where F_m is the maximum force reached during the test and β_{Rm} is a geometry dependent correlation coefficient which needs to be determined experimentally.

Besides this established method, the standard includes a different approach where R_m is directly calculated from the force F_i at a specific deflection u_i or displacement v_i on the SP curve:

$$R_m = \beta_{Rm} \frac{F_i}{h_0^2}, \tag{6}$$

The location u_i has been determined numerically and is largely independent from the tensile material properties [26]. It is associated with the onset of plastic instability. The correlation factor β_{Rm} has also been determined numerically and verified experimentally for a number of F/M steels [26]. Its values for the geometry and the two types of specimen in the standard are reproduced in Table 3.

Table 3. Parameters for Equation (3) as function of the SP test geometry and the curve type.

Geometry	***r* (mm)**	***D* (mm)**	**Lower die edge type**	$\mathbf{h_0}$ **(mm)**	**Curve type**	$\boldsymbol{u_i}$ **|** $\boldsymbol{v_i}$ **(mm)**	$\boldsymbol{\beta_{Rm}}$
Standard	1.25	4.0	Chamfer 0.2 x 45°	0.5	$F(u)$	0.552 (u_i)	0.192
Standard	1.25	4.0	Chamfer 0.2 x 45°	0.5	$F(v)$	0.645 (v_i)	0.179
Miniature	0.5	1.75	Chamfer 0.2 x 45°	0.25	$F(u)$	0.282 (u_i)	0.205
Miniature	0.5	1.75	Chamfer 0.2 x 45°	0.25	$F(v)$	0.320 (v_i)	0.197

5.3. Estimation of DBTT

The estimation of the ductile to brittle transition temperature (DBTT) was one of the main drivers for the development of the SP test method. The DBTT is the threshold temperature where the material behavior changes from brittle to ductile failure with rising temperature. The temperature at which the transition from brittle to ductile failure occurs is reflected in a rise of the fracture energy. The transition temperature T_{CVN} derived from the change of the absorbed energy in Charpy impact tests is often used as DBTT.

Similarly, an SP transition temperature T_{SP} can be determined from the force-deflection or the force-displacement curve. Many studies have shown that the transition temperatures from SP (T_{SP}) testing are much lower than from Charpy (T_{CVN}). The following relation is often used:

$$T_{SP} = \alpha T_{CVN}. \tag{7}$$

T_{SP} and T_{CVN} have to be expressed in absolute temperature. $\alpha \approx 0.4$ in many cases [3,7,27,28], although other values have been reported in some cases [27-29].

For determining T_{SP} the small punch energy E_{SP} needs to be calculated as a function of temperature. E_{SP} is the integral of the SP force-deflection curve:

$$E_{SP} = \int_0^{u_m} F(u)du. \tag{8}$$

Note that the upper integration limit is u_m, the deflection at maximum force as proposed in [30,31] (in contrast to the provisions in CWA 15627 according to which the integration is carried out up to a point where the force has dropped to 80% of its maximum). For the determination of T_{SP} it does not matter whether the integration is carried out over deflection u or displacement v. While the calculated energy values will change, this will not have a significant impact on T_{SP} itself.

In the case of brittle failure the SP curve can have some discontinuities where the force drops quasi-instantaneously because of cracking [5]. Such an event is referred to as pop-in (Figure 5). If an SP curve features pop-ins, the integration should be carried out up to the first significant pop-in, where a significant pop-in is defined as a force drop ΔF corresponding to 10% of the maximum force during the test [32]. The threshold of 10% was selected to be well above any noise level so it can be easily detected on the SP curve:

$$\Delta F = 0.1F_m. \tag{9}$$

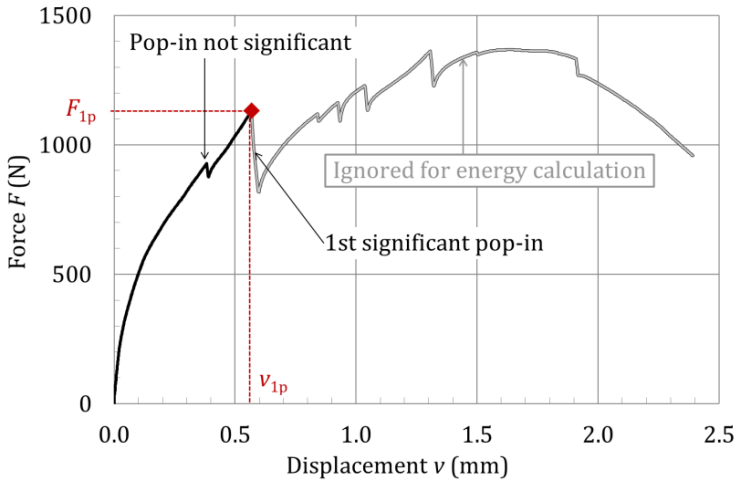

Figure 5. Force-displacement curve of a 13Cr-ODS-steel; energy calculation by integration up to the first significant pop-in.

Before determining T_{SP} from the E_{SP}(T) data it is useful to normalize E_{SP} by F_m as this leads to a constant level in the upper shelf [31]:

$$E_n = \frac{E_{SP}}{F_m}. \tag{10}$$

Then T_{SP} can be determined by performing a least square fit of the following equation to the data [31]:

$$E_n(T) = \frac{E_{US}+E_{LS}}{2} + \frac{E_{US}-E_{LS}}{2} tanh\left[\frac{T-T_{SP}}{C}\right], \tag{11}$$

where E_{US}, E_{LS}, C and T_{SP} are the fitting parameters. In this parametrization E_{US} and E_{LS} are the upper and lower shelf energies (normalized by F_m) i.e. the asymptotes of $E_n(T)$ for very high and low temperatures. Figure 6 shows an example of the T_{SP} determination.

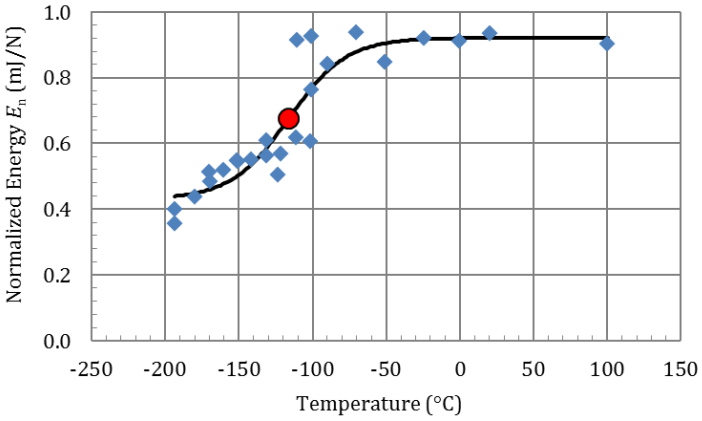

Figure 6. Determination of T_{SP} using the normalised energy E_n for steel P92; T_{SP} = -116 °C (circled symbol).

Alternatively, the DBTT can be estimated based on $T_{SP,\varepsilon}$, the SP transition temperature determined from the effective fracture strain ε_f. The effective fracture strain is defined as:

$$\varepsilon_f = ln\left[\frac{h_0}{h_f}\right], \tag{12}$$

where h_0 is the initial specimen thickness and h_f is the specimen thickness measured adjacent to the area of failure. h_f can be measured by cutting the specimen or non-destructively by techniques like 3D optical microscopy or X-ray computed tomography [31,32].

Once ε_f has been determined for a number of temperatures, $T_{SP,\varepsilon}$ can be calculated just as T_{SP} by fitting the function:

$$\varepsilon_f(T) = \frac{\varepsilon_{US}+\varepsilon_{LS}}{2} + \frac{\varepsilon_{US}-\varepsilon_{LS}}{2}\ tanh\left[\frac{T-T_{SP,\varepsilon}}{C'}\right]. \tag{13}$$

5.3. Estimation of fracture toughness

The significant differences in terms of specimen thickness, triaxiality or loading mode between conventional fracture toughness tests [34] and SP tests make the task of developing a methodology for estimating fracture properties complex. In this sense, the proposals included in the standard should be understood more as semi-quantitative approaches which, in any case can be used as a tool for screening criteria or as a valuable alternative to conventional tests in situations where it is impossible to machine standard fracture samples. On the other hand, it should be noted that the reliability of fracture toughness estimations by SP tests is on the order of magnitude of that achieved by correlations based on Charpy tests, which are widely accepted by in-use structural integrity codes [35].

Three options for the estimation of fracture toughness will be incorporated in the EN standard. The first one proposes to correlate the SP and Charpy transition temperatures (section 5.2) and then to use one of the existing correlations in literature [36] between the ductile-brittle Charpy transition temperature and K_{Ic} fracture toughness.

The second proposal estimates the fracture toughness in terms of J_{Ic}, by using the effective fracture strain, see equation (14).

$$J_{Ic} = k\varepsilon_f - J_0 \tag{14}$$

where k and J_0 are material-dependent fitting parameters.

The last of the methodologies included in the standard uses test pieces with a lateral notch (Figure 7). This notch allows any orientation of the material to be characterized, and, at the same time, allows the application of the principles of fracture mechanics, which require a pre-existing defect. The procedure for the estimation of the fracture resistance with this type of test specimen is based on the determination of the notch opening at the moment of cracking initiation. This value can be identified with the critical value of δ or CTOD of the material [37].

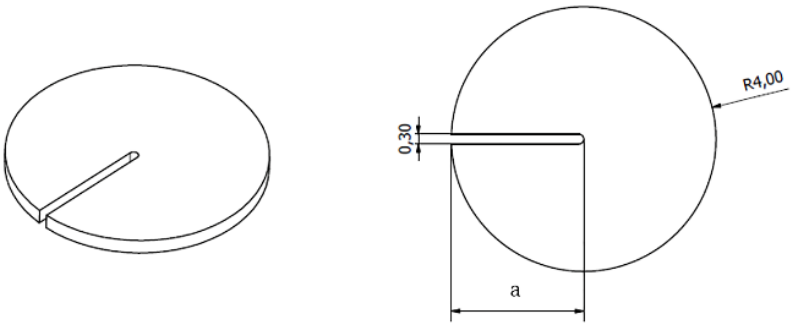

Figure 7. Notched test piece for fracture toughness estimation.

5.4. Estimation of creep properties

The main issue when using SPC data to estimate uniaxial creep properties is the conversion of the SPC force F to the uniaxial creep stress σ. The current CWA 15627 provides the following semi-empirical relation [20]:

$$\frac{F}{\sigma} = 3.33 k_{\mathrm{SP}} \frac{r^{1.2} h_0}{(0.5D)^{0.2}} \tag{15}$$

where r is the punch radius and D the diameter of the receiving hole. k_{SP} is a ductility related empirical correlation factor. However, k_{SP} does not only depend on the material but also on temperature [20,38] which limits its usefulness.

The soon to be published EN standard therefore includes a dedicated annex (annex G) which details a different approach in which the conversion from force to creep stress can be estimated through the "empirical force to stress conversion model" (EFS). The EFS (see Equation 16) was optimized by means of a large database from low alloy and 9Cr steels, such as 14MoV63, X20CrMoV121, P91, P92 and Eurofer-97, but also on a small data set of 316L stainless steel. The EFS force to stress ratio Ψ_{EFS} is given by:

$$\Psi_{\mathrm{EFS}} = \frac{F}{\sigma} = 1.916\, u_{\mathrm{min}}^{0.6579}\ [\mathrm{N/MPa}], \tag{16}$$

where u_{min} is the deflection at which the SPC deflection rate $\dot{u}$ reaches its minimum. The Ψ for the data set used for optimization is shown in Figure 8. It can be seen that the scatter in u_{min} can be substantial. The uniaxial test stresses corresponding to the SPC force at equal time to rupture have been log-linearly interpolated from uniaxial isothermal stress-time data [39, 40].

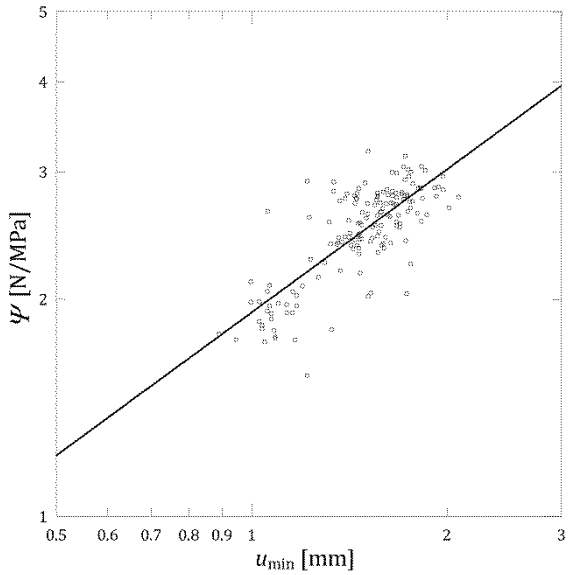

Figure 8. Relationship between Ψ_{EFS} (PSI) and the deflection u_{min} for a variety of steels tested at different organizations. Using the approach in eq. 15, Ψ would be constant and appear as a horizontal line.

In Figure 9 an SPC test curve for 316L stainless steel is shown together with a 3D profilometer scan of the ruptured specimen. The assessment of the SPC curve gives the following test specific values for equivalent stress and creep strain rate determination: t_r=14.3 h, $\dot{u}$ = 0.000231 mm/h, u_{min} =1.53 mm.

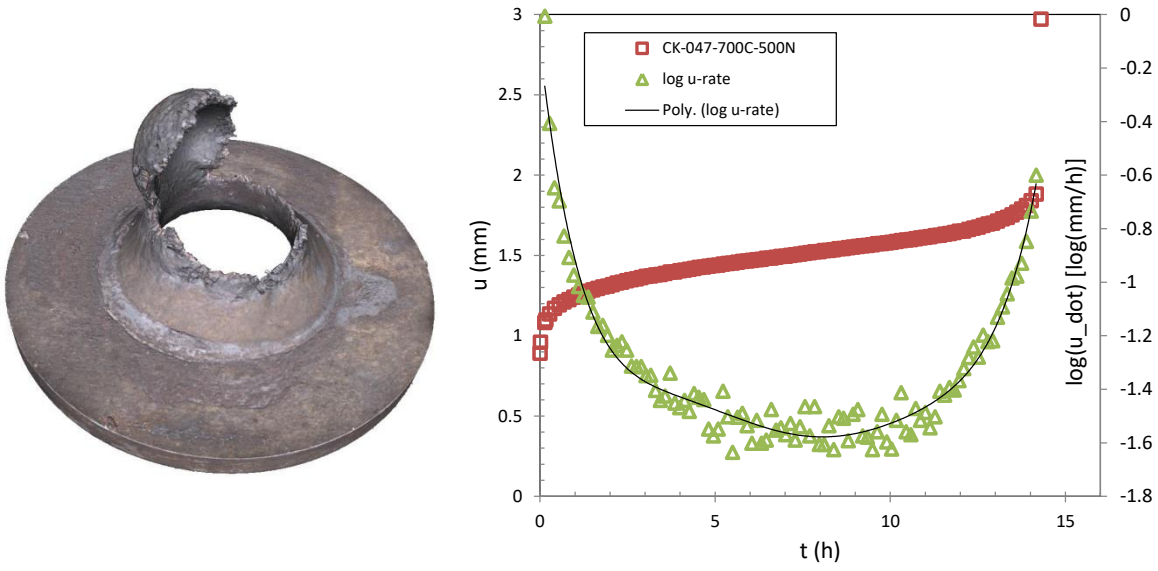

Figure 9. (a) 3D profilometer image of 316L SPC fracture (test CK-047 at 700°C / 500 N, t_r=14.3 h) [41]. Note ductile "hat" type fracture and **(b)** the corresponding time-deflection and deflection rate curves.

In Figure 10 uniaxial creep strength for a thick section forging steel (F92) is plotted against SPC equivalent stress at equal rupture times for equations 15 and 16. The "default value" k_{SP}=1 [20] used in equation 15 is appropriate for steels like P91 but not well suited for the softer F92 forging steel.

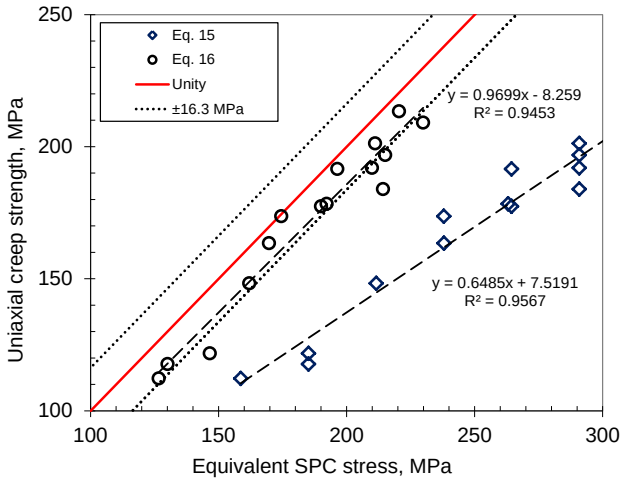

Figure 10. Equivalent SPC stress for F92 estimated by equations 15 and 16. Note that in equation 15 the default k_{SP} value 1 was used which works well for P91 and P92 steels but not for the softer F92.

Annex G also includes a formula for converting the measured minimum deflection rate to an equivalent minimum creep strain rate (equation 17). The equivalent minimum strain rate $\dot{\varepsilon}_{\min}$ (1/h) can be calculated from the minimum deflection rate $\dot{u}$ [mm/h] of an SPC test as:

$$\dot{\varepsilon}_{min} = 0.3922\dot{u}_{\min}^{1.191} \text{ [1/h]}. \quad (17)$$

The correlation between minimum deflection rate and minimum uniaxial strain rate is shown Figure 11.

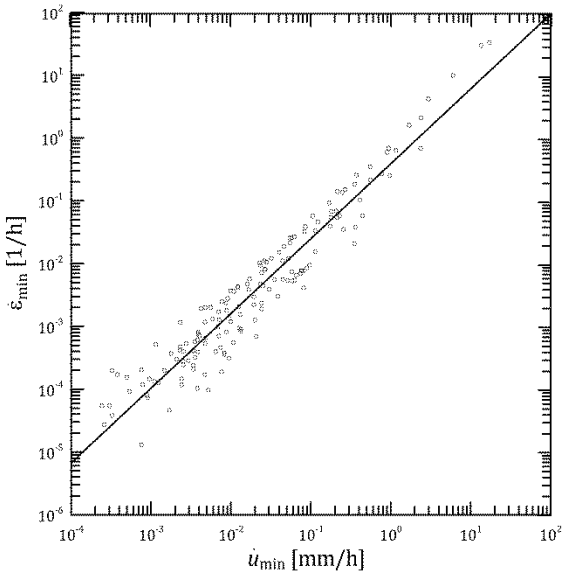

Figure 11. Relation between the minimum deflection rate $\dot{u}_{\min}$ and the minimum strain rate $\dot{\varepsilon}$.

6. Data Formats

With mechanical testing having the potential to produce large volumes of data of high inherent intellectual and commercial value, standardized formats offer the opportunity to transfer data efficiently and reliably between digital systems e.g. from test facility to database, database to data processing package, etc. In this context, data formats derived from mechanical testing standards for tensile, creep and fatigue testing have been developed in the scope of a series CEN Workshops on engineering materials data. The methodology relies on treating mechanical testing

standards as specifications from which a data model can be derived. This data model can then be implemented as a data format using the implementation technology of choice.

6.1. Examination of the documentary testing standard

In accordance with the methodology developed during the CEN Workshops on engineering materials data, examination of the EN 15627 small punch testing standard has yielded the structure and content of a corresponding data model, where structure refers to the hierarchical organization of categories of information and is derived primarily from an examination of the table of contents, while content means the fields that can be assigned values and is derived from a close examination of individual clauses. For both the structure and the content, the examination of the testing standard yields tables that map entries in the standard to features in the model. The structural features of the EN 15627 data model are listed in Table 4.

Table 4. Structural features of the EN 15627 data model.

Source	URI
[EN 15627] EN Standard title.	sp
[EN 15627, 8.4 and 9.5] Clause title.	sp:test_report
[EN 15627, 6] First paragraph.	sp:test_report:test_piece
[EN 15627, 6] Table 6.1.	sp:test_report:test_piece:dimensions
[EN 15627, 8.2 and 9.3] Clause title.	sp:test_report:procedure
[EN 15627, 4] Term 4.1.	sp:test_report:procedure:punch
[EN 15627, European Forward] Paragraph 2.	sp:test_report:results
[EN 15627, 2] First paragraph.	sp:test_report:results:properties
[EN 15627, 8.4 and 9.5] Sixth list item.	sp:test_report:results:curve

In turn and as shown in Figure 10, the information in the mapping tables can be presented graphically.

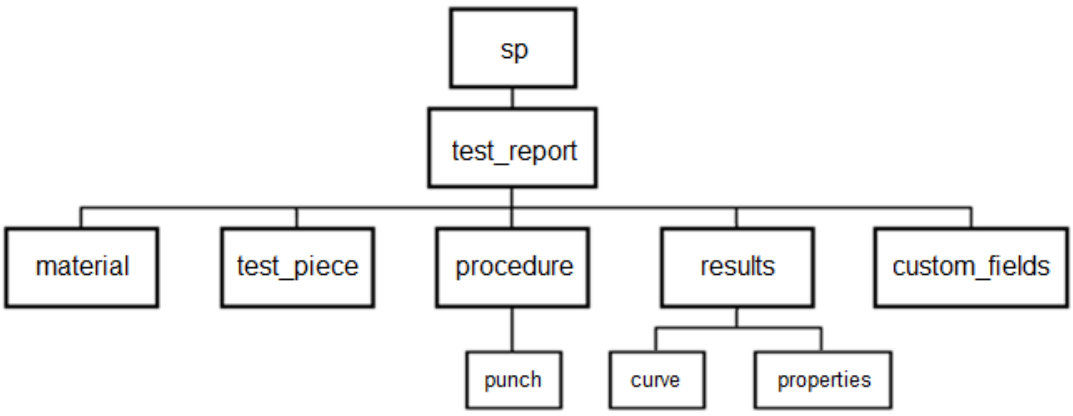

Figure 12. Structural features of the EN 15627 data model.

Having established the structure, the preliminary content is determined from an examination of the vocabulary and symbols clauses, with subsequent examination of the remaining clauses allowing the content to be fully elaborated. Again, this procedure results in tables and figures similar to those of Figure 12 and Table 4, respectively.

This methodology has been applied to EN 15627, yielding an XSD (XML Schema Definition) data format that is intended to be made available from http://uri.cen.eu and referenced from the standard.

7. Conclusions

The new EN standard on SP testing of metallic materials defines the test rig and the procedures for carrying out SP and SPC tests from cryogenic to high temperatures. These provisions are largely consistent with the current CWA 15627. Notable modifications in the new standard are the alignment of the punch diameter between SP and SPC tests and the harmonization of the used symbols. Besides the most frequently used specimen, the new standard will allow using a miniaturized TEM sample sized specimen.

In its informative annexes the new standard provides guidance for the estimation of tensile, fracture mechanical and creep material properties. In particular for the estimation of ultimate tensile strength R_m and the creep properties the recommendations differ from the provisions in CWA 15627. While the recommended methods for estimating $R_{p0.2}$, DBTT and fracture toughness mostly follow those in CWA 15627, they are described in more detail and differ in some points.

The new standard includes the definition of a standard data format to make the test results machine readable and will simplify the exchange of test data between different electronic systems and organizations.

At the time of writing the comments from ECISS/TC101 on the draft standard have been received and implemented. The public enquiry period is expected to start early this summer. Depending on the outcome of the public enquiry, the publication of the final standard can be expected in the course of 2019.

Acknowledgments

The authors gratefully acknowledge the support of the other members of ECISS/TC101/WG1.

Swansea University's participation in ECISS/TC101/WG1 was supported by the EPSRC Rolls-Royce Strategic Partnership in Structural Metallic Systems for Gas Turbines (grants EP/H500383/1 and EP/H022309/1).

References

1. Lucas G., The development of small specimen mechanical test techniques, *Journal of Nuclear Materials*, **1983**, *117*, 327–339, https://doi.org/10.1016/0022-3115(83)90041-7
2. Manahan M.P.; Argon A.S.; Harling O.K., The development of a miniaturized disk bend test for the determination of postirradiation mechanical properties. *Journal of Nuclear Materials*, **1981**, *103 & 104*,1545-1550, https://doi.org/10.1016/0022-3115(82)90820-0
3. Baik J.-M.; Kameda J.; Buck O., Small punch test evaluation of intergranular embrittlement of an alloy steel. *Scripta Metallurgica*, **1983**, *17*,1443-1447, https://doi.org/10.1016/0036-9748(83)90373-3
4. Misawa T.; Sugawara H.; Miura R.; Hamaguchi Y., Small specimen fracture toughness tests of HT-9 steel irradiated with protons, *Journal of Nuclear Materials*, **1985**, *133-134*, 313-316, https://doi.org/10.1016/0022-3115(85)90158-8
5. Kameda J.; Buck O., Evaluation of the ductile-to-brittle transition temperature shift due to temper embrittlement and neutron irradiation by means of a small-punch test, *Materials Science and Engineering*, **1986**, *83(1)*, 29-38, https://doi.org/10.1016/0025-5416(86)90171-0
6. Mao X.; Takahashi H., Development of a further-miniaturized specimen of 3 mm diameter for tem disk (ø 3 mm) small punch tests, *Journal of Nuclear Materials*, **1987**, *150(1)*, 42-52, https://doi.org/10.1016/0022-3115(87)90092-4
7. Misawa T.; Adachi T.; Saito M.; Hamaguchi Y, Small punch tests for evaluating ductile-brittle transition behavior of irradiated ferritic steels, *Journal of Nuclear Materials*, **1987**, *150(2)*, 194-202, https://doi.org/10.1016/0022-3115(87)90075-4
8. Kopriva R., Eliasova I., Kytka M., Implementation of Small Punch Testing and Automated Ball Indentation in the Process of Irradiated NPP Materials Degradation Evaluation. ASME. International Conference on Nuclear Engineering, **2016**, *Volume 5: Student Paper Competition* ():V005T15A043, https://doi.org/10.1115/ICONE24-60620
9. Petzová J.; Březina M.; Kapusňák M.; Kupča L., Application of small punch testing methods for thermal ageing monitoring at primary circuit components in nuclear power plant. *Proceedings of ASME Pressure Vessels and Piping Division Conference*, **2015**, *Vol. 1A*, https://doi.org/10.1115/PVP2015-45539
10. Hurst R.; Lancaster R.J.; Jeffs S.P.; Bache M.R., The contribution of small punch testing towards the development of materials for aero-engine applications, *Theoretical and Applied Fracture Mechanics*, **2016**, *86, Part A*,

11. Lancaster R.J.; Illsley H.W.; Davies G.R.; Jeffs S.P.; Baxter G.J., Modelling the small punch tensile behaviour of an aerospace alloy, *Materials Science and Technology (United Kingdom)*, **2017**, *33(9)*, 1065-1073, https://doi.org/10.1080/02670836.2016.1230168
12. Fernández M.; Rodríguez C; Belzunce F.J; García T.E., Use of small punch test to estimate the mechanical properties of sintered products and application to synchronizer hubs, *Metal Powder Report*, **2017**, 72(5), https://doi.org/10.1016/j.mprp.2016.02.056
13. Walters C.L.; Bruchhausen M.; Lapetite J.-M.; Duvalois W., Fracture Testing of Existing Structures Without the Need for Repairs. *ASME. International Conference on Offshore Mechanics and Arctic Engineering*, **2017**, *Volume 4: Materials Technology* ():V004T03A027. https://doi:10.1115/OMAE2017-61420
14. Rodríguez C.; Cuesta I.I.; Maspoch M.L.L.; Belzunce F.J, Application of the miniature small punch test for the mechanical characterization of polymer materials, *Theoretical and Applied Fracture Mechanics*, **2016**, *86*, 78-83, https://doi.org/10.1016/j.tafmec.2016.10.001
15. Singh J., Sharma N.K., Sehgal S.S.; Small Punch Testing: an alternative testing technique to evaluate tensile behavior of cortical bone, *Journal of Mechanics in Medicine and Biology*, **2017**, 17(6), https://doi.org/10.1142/S0219519417501020
16. Standards Press of China (SPC), *Small punch test methods of metallic materials for in-service pressure equipments – part 1: General requirements*, 2012, GB/T 29459.1– 012.
17. Standards Press of China (SPC), *Small punch test methods of metallic materials for in-service pressure equipments – part 2: Method of test for tensile properties at room temperature*, 2012, GB/T 29459.2–2012.
18. The Society of Materials Science, *Standard for small punch creep test – estimation of residual life for high temperature component*. Japan, 2012, ISBN 978-4-901381-38-3.
19. ASTM WK 61832, New practice for Small Punch test method for metallic materials on https://www.astm.org/DATABASE.CART/WORKITEMS/WK61832.htm (accessed on 27 March 2018)
20. European Committee for Standardization, *Small punch test method for metallic materials*, 2007, CEN Workshop Agreement, CWA 15627:2007 E.
21. Lancaster R.; Davies G.; Illsley H.; Jeffs S.; Baxter G., Structural integrity of an electron beam melted titanium alloy, *Materials*, **2016**, *9(6)*, p. 470, https://doi:10.3390/ma9060470
22. de Weerd W.; Bruchhausen M., Small punch tensile/fracture test data for AISI 316L ar material at 20 °C and a displacement rate of .00833 mm/s (fifth repeat test), version 1.0, European Commission JRC, [Dataset], http://dx.doi.org/10.5290/2700156
23. Lapetite J.-M.; Holmström S.; Bruchhausen M., Small punch creep test data for P92 ar material at 625 °C and a load of 375 N, **2016**, version 1.3, European Commission JRC, [Dataset], http://dx.doi.org/10.5290/2700101
24. Bruchhausen M.; Holmström S.; Simonovski I.; Austin T.; Lapetite J.-M.; Ripplinger S.; de Haan, F., Recent developments in small punch testing: Tensile properties and DBTT, *Theoretical and Applied Fracture Mechanics*, **2016**, *86*, 2–10, https://doi.org/10.1016/j.tafmec.2016.09.012
25. García T.E.; Rodríguez C.; Belzunce F.J.; Suárez C., Estimation of the mechanical properties of metallic materials by means of the small punch test, *Journal of Alloys and Compounds*, **2014**, *582*, 708-717, https://doi.org/10.1016/j.jallcom.2013.08.009
26. Altstadt E.; Houska M.; Simonovski I.; Bruchhausen M.; Holmström S.; Lacalle R., On the estimation of ultimate tensile stress from small punch testing, *International Journal of Mechanical Sciences*, **2018**, *136*, 85-93, https://doi.org/10.1016/j.ijmecsci.2017.12.016
27. Kameda J., A kinetic model for ductile-brittle fracture mode transition behavior, *Acta metallurgica*, **1986**, *34(12)*, 2391-2398, https://doi.org/10.1016/0001-6160(86)90142-2
28. Turba K.; Hurst R; Hähner P.; Evaluation of the ductile–brittle transition temperature in the NESC-I material using small punch testing, *International Journal of Pressure Vessels and Piping*, **2013**, *111-112*, 155-161, https://doi.org/10.1016/j.ijpvp.2013.07.001
29. Contreras M.A.; Rodríguez C.; Belzunce F.J.; Betegón C. Use of the small punch test to determine the ductile-to-brittle transition temperature of structural steels. *Fatigue & Fracture of Engineering Materials & Structures*, **2008**, *31*,727-737, https://doi.org/10.1111/j.1460-2695.2008.01259.x
30. Altstadt E., Ge H.E., Kuksenko V., Serrano M., Houska M., Lasan M., Bruchhausen M., Lapetite J.-M., Dai Y., 2016. Critical evaluation of the small punch test as a screening procedure for mechanical properties. *Journal of Nuclear Materials*, **2016**, 472, 186–195, https://doi.org/10.1016/j.jnucmat.2015.07.029

31. Bruchhausen M.; Holmström S., Lapetite J.-M.; Ripplinger S., On the determination of the ductile to brittle transition temperature from small punch tests on Grade 91 ferritic-martensitic steel, *International Journal of Pressure Vessels and Piping*, **2017**, *155*, 27-34, https://doi.org/10.1016/j.ijpvp.2017.06.008
32. Altstadt E., Serrano M., Houska M., García-Junceda A., 2016. Effect of anisotropic microstructure of a 12Cr-ODS steel on the fracture behaviour in the small punch test. *Materials Science and Engineering: A*, **2016**, 654, 309–316, https://doi.org/10.1016/j.msea.2015.12.055
33. Bruchhausen M.; Lapetite J.-M.; Ripplinger S.; Austin, T., Small punch tensile/fracture test data and 3D specimen surface data on Grade 91 ferritic/martensitic steel from cryogenic to room temperature, *Data in Brief*, **2016,** *9*, 245-251, https://doi.org/10.1016/j.dib.2016.08.061
34. ASTM E 1820-17, Standard Test Method for Measurement of Fracture Toughness, *Annual Book of ASTM Standards*, 2017.
35. BS7910:2013, Guide to methods for assessing the acceptability of flaws in metallic structures, BSI, 2013.
36. Shekhter A.; Croker A.B.L.; Hellier A.K.; Moss C.J.; Ringer S.P., Towards the Correlation of Fracture Toughness in an Ex-Service Power Generation Rotor, *International Journal of Pressure Vessels and Piping*, **2000**, *77*, 113-116, https://doi.org/10.1016/S0308-0161(99)00091-5
37. Lacalle R.; Álvarez J.A.; Arroyo B.; Gutiérrez-Solana F., Methodology for fracture toughness estimation based on the use of Small punch notched specimens and the CTOD concept, In: The 2nd International Conference SSTT 2012, Conference Proceedings, October 2012.
38. Holmström S.; Hähner P.; Hurst R.; Bruchhausen M.; Fischer B.; Lapetite J.-M.; Gupta M., 2014. Small punch creep testing for material characterization and life time prediction". In 10th Liege Conference: Materials for Advanced Power Engineering 2014, Lecomte-Beckers J.; Dedry O.; Oakey J.; Kuhn. B, (eds.), 627–635.
39. Holmström S.; Li Y.; Dymacek P.; Vacchieri E.; Jeffs S.; Lancaster R.; Omacht D.; Zdenek K.; Anelli E.; Rantala J.; Tonti A.; Komazaki S.; Narveena; Bruchhausen M.; Hurst R.; Hähner P.; Richardson M.; Andres D., Creep strength and minimum strain rate estimation from Small Punch Creep tests, *Materials Science & Engineering A* (under review)
40. Dymáček P., Li Y., Dobeš F., Stevens P., New approach to determination of uniaxial creep properties from small punch creep curves, Materials at High Temperatures (under review)
41. Lapetite J-M; Holmström S; Bruchhausen M, Small punch creep test data for AISI 316L ar material at 700 °C and a load of 500 N, **2018**, version 1.0, European Commission JRC, [Dataset], http://dx.doi.org/10.5290/2700158